

Effect of Particulate Debonding in AA5050/Boron Nitride Nanoparticulate Reinforced Metal Matrix Composites

¹H. B. Niranjan and A. Chennakesava Reddy²

¹Associate Professor, Department of Mechanical Engineering, M.S.R.I.T, Bangalore, India

²Assistant Professor, Department of Mechanical Engineering, MJ College of Engineering and Technology, Hyderabad, India
dr_acreddy@yahoo.com

Abstract: A square array unit cell/2-D octahedrons particulate RVE models were employed to evaluate interfacial debonding using cohesive zone analysis. The particulate metal matrix composites are boron nitride/AA5050 alloy at volume fractions of 10%, 20% and 30% boron nitride. Interface debonding was observed in all the composites.

Keywords: AA5050 alloy, boron nitride, octahedron particulate, RVE model, finite element analysis, interface debonding.

1. INTRODUCTION

Interface adhesion, cohesion and friction are important in micromechanics of composites. Material interfaces are considered to exhibit tensile bond and shear resistance at the macroscopic continuum level. The notion of a zero-thickness interface results in elastic stiffness properties which relate surface tractions to relative displacements. A traction-separation based constitutive response is defined by an adhesive material with number of material parameters including interfacial penalty stiffness, interfacial strength, and the critical energy [1-2]. Damage initiation takes place as the degradation of the stiffness begins when the stresses and/or strains satisfy a specified damage initiation criterion. Numerical simulations were carried out on the interface between the particulate and matrix to obtain a traction–separation relationship [3-16].

The present study considers the deformation of the interface between AA5050 alloy and boron nitride nanoparticle. Representative volume elements (RVEs) models were taken from the periodic 2-D octahedron particulates in a square array distribution (figure 1).

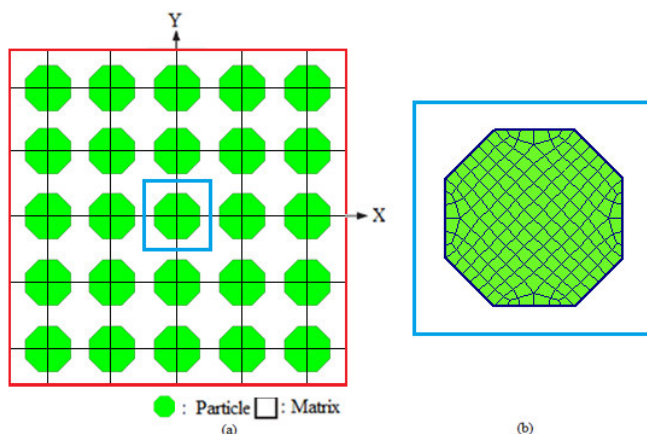


Figure 1: The RVE model.

2. MATERIALS AND METHODS

The computational domain considered in the current research is comprised of AA5050 alloy matrix material with an embedded 2-D octahedron boron nitride inclusion. The volume fractions of boron nitride were 10%, 20%, and 30%. In the model periodic boundary conditions were used in the x and y directions. Initially, both AA5050 and boron nitride were kept in contact along the interface in the x–y plane with zero separation distance. The simulation domain is divided into three regions: Boron nitride nanoparticle, interface and AA505 alloy matrix. PLANE183 element was used for the matrix and the nanoparticulates. The cohesive zone can be incorporated in the continuum formulation by applying the cohesive tractions as boundary conditions. The cohesive element is implemented as a linear element with four nodes. Initially, the interface between the matrix material and the inclusion is assumed to be perfectly bonded, that is, continuity of traction and displacement is assumed along the interface.

The finite element analysis was carried out for the single inclusion model undergoing a tensile load. The elastic material properties are given by $E_m = 68.90$ GPa, $E_p = 100$ GPa, $\nu_m = 0.33$ and $\nu_p = 0.27$.

Shear-log model is based on the assumption that all of the load transfer from matrix to particulate occurs via shear stresses acting on the particulate interface between the two constituents. The rate of change of the stress in the particulate to the interfacial shear stress at that point and the particulate radius, 'r' is given by:

$$\frac{d\sigma_p}{dx} = -\frac{2\tau_i}{r} \quad (1)$$

which may be regarded as the basic shear lag relationship.

The stress distribution in the particulate is determined by relating shear strains in the matrix around the particulate to the macroscopic strain of the composite. Some mathematical manipulation leads to a solution for the distribution of stress at a distance 'x' from the mid-point of the particulate which involves hyperbolic trig functions:

$$\sigma_p = E_p \varepsilon_c [1 - \cosh(nx/r) \operatorname{sech}(ns)] \quad (2)$$

where ε_c is the composite strain, s is the particulate aspect ratio (length/diameter) and n is a dimensionless constant given by:

$$n = \left[\frac{2E_m}{E_p(1+\nu_m)\ln(1+\nu_p)} \right]^{1/2} \quad (3)$$

in which ν_m is the Poisson ratio of the matrix. The variation of interfacial shear stress along the particulate length is derived, according to Equation (1), by differentiating this equation, to give:

$$\tau_i = \frac{n\varepsilon_c}{2} E_p \sinh\left(\frac{nx}{r}\right) \operatorname{sech}(ns) \quad (4)$$

The equation for the stress in the particulate, together with the assumption of a average tensile strain in the matrix equal to that imposed on the composite, can be used to evaluate the composite stiffness. This leads to:

$$\sigma_c = \varepsilon_c \left[\nu_p E_p \left(1 - \frac{\tanh(ns)}{ns}\right) + (1 - \nu_p) E_m \right] \quad (5)$$

The expression in square brackets is the composite stiffness. The stiffness is a function of particulate aspect ratio, particulate/matrix stiffness ratio and particulate volume fraction.

If the particle deforms in an elastic manner (according to Hooke's law) then,

$$\tau = \frac{n}{2} \sigma_p \quad (6)$$

If interfacial debonding/yielding is considered to occur when the interfacial shear stress reaches its shear strength

$$\tau = \tau_{\max} \quad (7)$$

For particle/matrix interfacial fracture can be established whereby,

$$\tau_{\max} < \frac{n\sigma_p}{2} \quad (8)$$

This approach suggests that the outcome of a matrix crack impinging on an embedded particle depends on the balance between the particle strength and the shear strength of the interface. For plane strain conditions, the macro stress- macro strain relation is as follows:

$$\begin{Bmatrix} \bar{\sigma}_x \\ \bar{\sigma}_y \\ \bar{\tau}_{xy} \end{Bmatrix} = \begin{bmatrix} \bar{C}_{11} & \bar{C}_{12} & 0 \\ \bar{C}_{21} & \bar{C}_{22} & 0 \\ 0 & 0 & \bar{C}_{33} \end{bmatrix} \times \begin{Bmatrix} \bar{\varepsilon}_x \\ \bar{\varepsilon}_y \\ \bar{\gamma}_{xy} \end{Bmatrix} \quad (9)$$

The interfacial tractions can be obtained by transforming the micro stresses at the interface as given in Eq. (3):

$$t = \begin{Bmatrix} t_z \\ t_n \\ t_t \end{Bmatrix} = T\sigma \quad (10)$$

$$\text{where, } T = \begin{bmatrix} 0 & 0 & 0 \\ \cos^2\theta & \sin^2\theta & 2\sin\theta\cos\theta \\ -\sin\theta\cos\theta & \sin\theta\cos\theta & \cos^2\theta - \sin^2\theta \end{bmatrix}$$

3. RESULTS AND DISCUSSION

The tensile modulus decreased with volume fraction of boron nitride as shown figure 2a. The shear modulus was nearly constant with increase in the volume fraction of boron nitride in the composites (figure 2b). The major Poisson's ratio decreased with volume fraction of boron nitride. The stiffness mismatch between boron nitride nanoparticulate and AA5050 alloy matrix is 31 GPa. The condition $\tau_{\max} < n\sigma_p/2$ is satisfied for the incidence of debonding in the composites including 10%, 20% and 30% boron nitride (figure 3). The shear stresses induced in the composites are shown in figure 4. For the

shearing of interface between the boron nitride inclusion and AA5050 alloy matrix, the shear stress increased with increase of boron nitride inclusion in AA5050 alloy matrix.

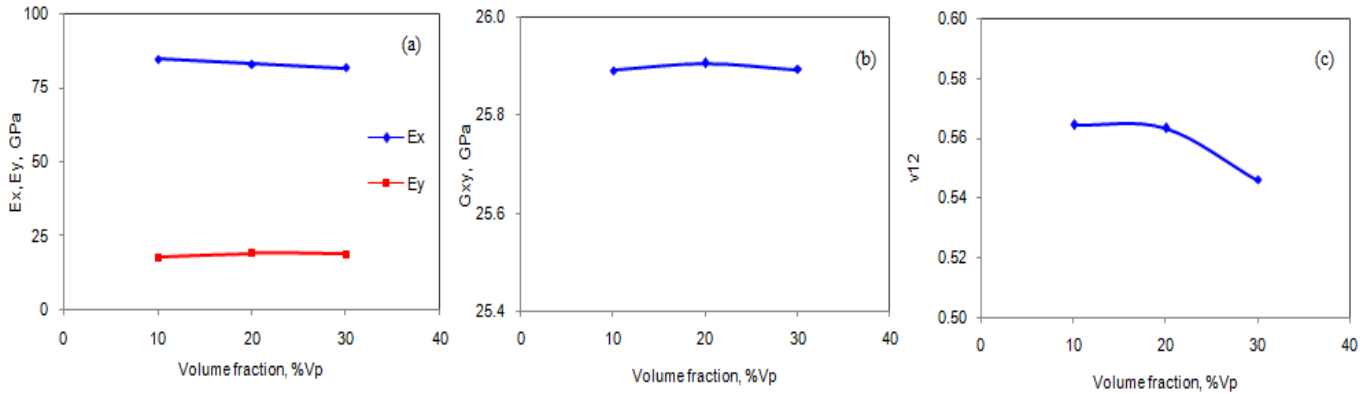


Figure 2: Effect of volume fraction on effective material properties.

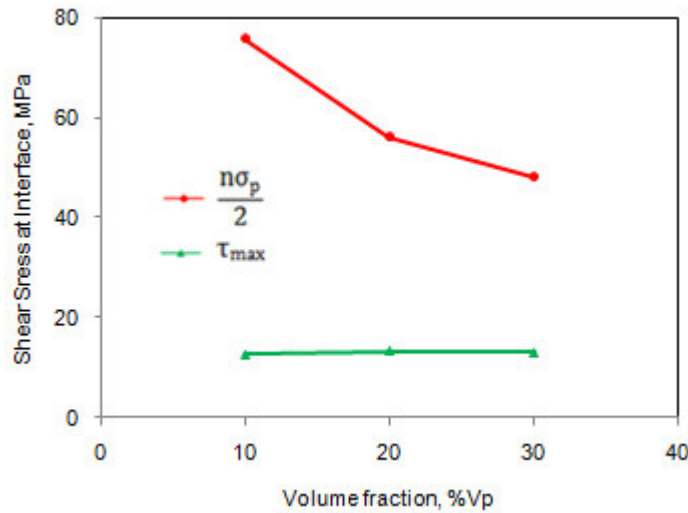


Figure 3: Fracture criteria of interface debonding.

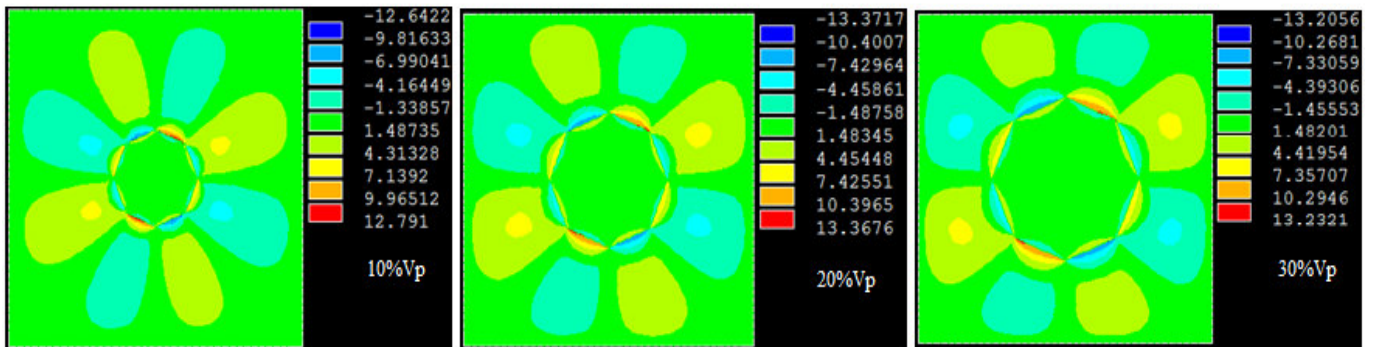


Figure 4: Effect of volume fraction on shear strength.

The normal and tangential tractions are plotted in figure 5. Because of symmetry considerations, the variations of the interface stresses with circumferential location are plotted only for the range $0^\circ \leq \theta \leq 90^\circ$. As these stresses were calculated locally near the interface they therefore relate to the traction–separation law. The normal traction in the region of interface between boron nitride nanoparticulate and AA5050 alloy matrix was constant with increase of volume fraction of boron nitride. The plots shown are for the normal and tangential traction dominated failure. The maximum allowable normal and tangential separation of the cohesive element corresponds to the separation distance at which the traction decreases to near zero value.

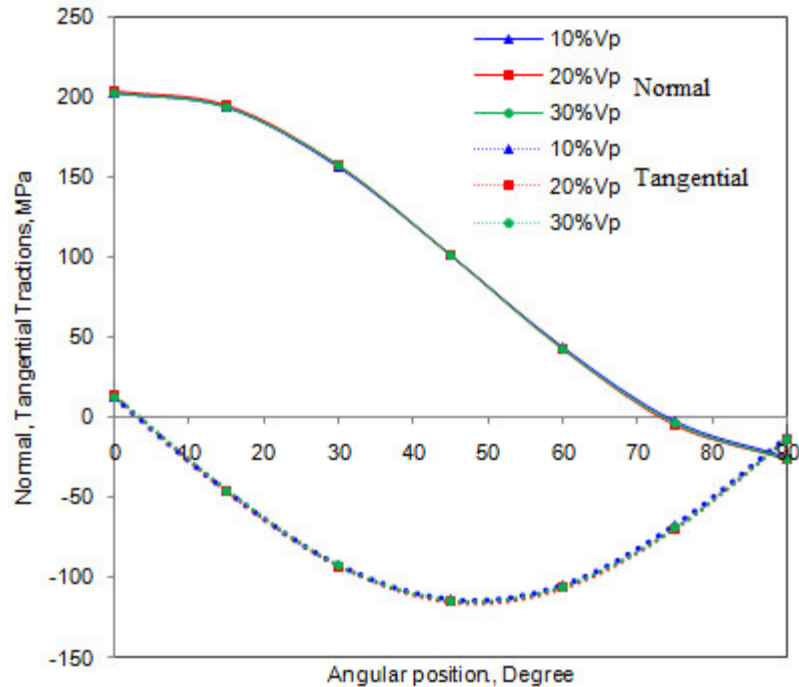


Figure 5: Normal and tangential: (a) tractions and (b) displacements.

4. CONCLUSION

The interface debonding occurred in the composites containing 10%, 20% and 30% volume fractions boron nitride. As these stresses were calculated locally near the interface they therefore relate to the traction in the traction–separation law. The maximum allowable normal and tangential separation of the cohesive element corresponds to the separation distance at which the traction decreases to near zero value.

REFERENCES

1. M. Elices, G. V. Guinea, J. Gomez, J. Planas, The cohesive zone model: advantages, limitations and challenges, *Engineering Fracture Mechanics*, 69, 2002, pp.137–163.
2. A. Needleman, An analysis of decohesion along an imperfect interface. *International Journal of Fracture*, 42, 1990, pp. 21-40.
3. A. Chennakesava Reddy, Assessment of Debonding and Particulate Fracture Occurrences in Circular Silicon Nitride Particulate/AA5050 Alloy Metal Matrix Composites, National Conference on Materials and Manufacturing Processes, Hyderabad, India, 27-28 February 1998, pp.104-109.
4. B. Kotiveera Chari and A. Chennakesava Reddy, Numerical Simulation of Particulate Fracture in Round Silicon Nitride Particulate/AA6061 Alloy Metal Matrix Composites, National Conference on Materials and Manufacturing Processes, Hyderabad, India, 27-28 February 1998, pp. 110-114.
5. H. B. Niranjan and A. Chennakesava Reddy, Effect of Elastic Moduli Mismatch on Particulate Fracture in AA7020/Silicon Nitride Particulate Metal Matrix Composites, National Conference on Materials and Manufacturing Processes, Hyderabad, India, 27-28 February, 1998, pp. 115-118,
6. P. Martin Jebaraj and A. Chennakesava Reddy, Cohesive Zone Modelling for Interface Debonding in AA8090/Silicon Nitride Nanoparticulate Metal Matrix Composites, National Conference on Materials and Manufacturing Processes, Hyderabad, India, 27-28 February 1998, pp. 119-122.
7. P. Martin Jebaraj and A. Chennakesava Reddy, Plane Strain Finite Element Modeling for Interface Debonding in AA1100/Silicon Oxide Nanoparticulate Metal Matrix Composites, National Conference on Materials and Manufacturing Processes, Hyderabad, India, 27-28 February 1998, pp. 123-126.
8. A. Chennakesava Reddy, Local Stress Differential for Particulate Fracture in AA2024/Titanium Carbide Nanoparticulate Metal Matrix Composites, National Conference on Materials and Manufacturing Processes, Hyderabad, India, 27-28 February 1998, pp. 127-131.
9. B. Kotiveera Chari and A. Chennakesava Reddy, Interface Debonding and Particulate Fracture based on Strain Energy Density in AA3003/MgO Nanoparticulate Metal Matrix Composites, National Conference on Materials and Manufacturing Processes, Hyderabad, India, 27-28 February 1998, pp. 132-136.
10. H. B. Niranjan and A. Chennakesava Reddy, Numerical and Analytical Prediction of Interface Debonding in AA4015/Boron Nitride Nanoparticulate Metal Matrix Composites, National Conference on Materials and Manufacturing Processes, Hyderabad, India, 27-28 February 1998, pp. 137-140.

11. S. Sundara Rajan and A. Chennakesava Reddy, Effect of Particulate Volume Fraction on Particulate Cracking in AA5050/Zirconium Oxide Nanoparticulate Metal Matrix Composites , National Conference on Materials and Manufacturing Processes, Hyderabad, India, 27-28 February 1998, pp. 156-159.
12. S. Sundara Rajan and A. Chennakesava Reddy, Cohesive Zone Analysis for Interface Debonding in AA6061/Titanium Nitride Nanoparticulate Metal Matrix Composites , National Conference on Materials and Manufacturing Processes, Hyderabad, India, 27-28 February 1998, pp. 160-164.
13. A. Chennakesava Reddy, Effect of Particle Loading on Microelastic Behavior and interfacial Traction of Boron Carbide/AA4015 Alloy Metal Matrix Composites, 1st International Conference on Composite Materials and Characterization, Bangalore, 14-15 March 1997, pp. 176-179.
14. A. Chennakesava Reddy, Reckoning of Micro-stresses and interfacial Traction in Titanium Boride/AA2024 Alloy Metal Matrix Composites, 1st International Conference on Composite Materials and Characterization, Bangalore, 14-15 March 1997, pp. 195-197.
15. A. Chennakesava Reddy, Interfacial Debonding Analysis in Terms of Interfacial Traction for Titanium Boride/AA3003 Alloy Metal Matrix Composites, 1st National Conference on Modern Materials and Manufacturing , Pune, India, 19-20 December 1997, pp. 124-127.
16. A. Chennakesava Reddy, Evaluation of Debonding and Dislocation Occurrences in Rhombus Silicon Nitride Particulate/AA4015 Alloy Metal Matrix Composites, 1st National Conference on Modern Materials and Manufacturing , Pune, India, 19-20 December 1997, pp. 278-282.